Hindawi Publishing Corporation
International Journal of Photoenergy
Volume 2013, Article ID 392408, 6 pages
http://dx.doi.org/10.1155/2013/392408

Research Article

Tailoring the Spectra of White Organic Light-Emitting Devices by Trap Effect of a Concentration-Insensitive Dopant

Qi Wang,[1] Junsheng Yu,[1] Ming Li,[2] and Zhiyun Lu[2]

[1] *State Key Laboratory of Electronic Thin Films and Integrated Devices, School of Optoelectronic Information, University of Electronic Science and Technology of China (UESTC), Chengdu 610054, China*
[2] *College of Chemistry, Sichuan University, Chengdu 610064, China*

Correspondence should be addressed to Junsheng Yu; jsyu@uestc.edu.cn

Received 3 November 2012; Accepted 3 January 2013

Academic Editor: K. R. Justin Thomas

Highly efficient phosphorescent organic light-emitting devices (PhOLEDs) had been fabricated by using a novel iridium complex, bis[2-(3′,5′-di-tert-butylbiphenyl-4-yl)benzothiazolato-N,$C^{2'}$]iridium(III) (acetylacetonate) [$(tbpbt)_2Ir(acac)$], as the emitter. With a wide doping ratio ranging from 15 wt% to 25 wt%, the PhOLEDs maintained a comparable high performance, indicating concentration-insensitive property of the $(tbpbt)_2Ir(acac)$. On the basis of the unique characteristic of concentration insensitivity, the application of this phosphor was explored by fabricating white organic light-emitting devices (WOLEDs) with altered doping ratio, indicating that trap effect of $(tbpbt)_2Ir(acac)$ could effectively tailor WOLEDs spectra. Typically, a high-power efficiency, current efficiency, and external quantum efficiency of 30.0 lm/W, 38.8 cd/A, 18.1%, were achieved by 20 wt% doped WOLEDs.

1. Introduction

White organic light-emitting diodes (WOLEDs) have drawn considerable attentions in recent years due to their great promise to enhance energy efficiency, when serving as the backlight in flat-panel displays and the highly potential candidate for next generation of large area solid state lighting [1, 2]. Generally, for realizing high-efficiency WOLED, one of the most important factors is that most of the singlet and triplet excitons should be efficiently utilized for light emission [3]. Given this, WOLEDs employing iridium chelate phosphors have drawn considerable interest in recent years, since they could harness two kinds of excitons to yield a theoretical internal quantum efficiency of 100% [4]. Till now, to achieve high-efficient phosphorescent WOLEDs, many efforts, such as inserting charge blocking layers, varying layer thicknesses and adjusting doping concentrations, have been introduced to tune charge carrier recombination and exciton utilization [4–7]. Consequently, complementary (e.g., blue and orange) or primary colors (red, green, and blue) could be balanced to give off efficient white emission. Among these strategies, the technique of adjusting dopant ratio is widely applied as an effective method to tune emission color and device efficiency. However, since two key factors, that is, efficiency and spectrum, need to be taken into account for high-performance WOLEDs, the optimization of color quality and device efficiency is not always realized simultaneously. Typically, efficient and bright devices are not white enough, while white devices are not sufficiently efficient. This problem is especially intractable when the emitters used in WOLEDs are concentration-sensitive phosphors, where slight variation on doping ratio usually leads to a dramatic alteration of device performance. As a result, a large amount of endeavor must be attempted to compromise the device efficiency/color quality tradeoffs, which will prolong research time, multiply experimental complexity, and raise the overall production cost.

One straightforward resolution for this problem lies in the synthesis of novel phosphorescent iridium complexes, which could maintain high efficiency with a wide range of doping ratio. Therefore, the device spectra could be adjusted independently without necessarily sacrificing device efficiency.

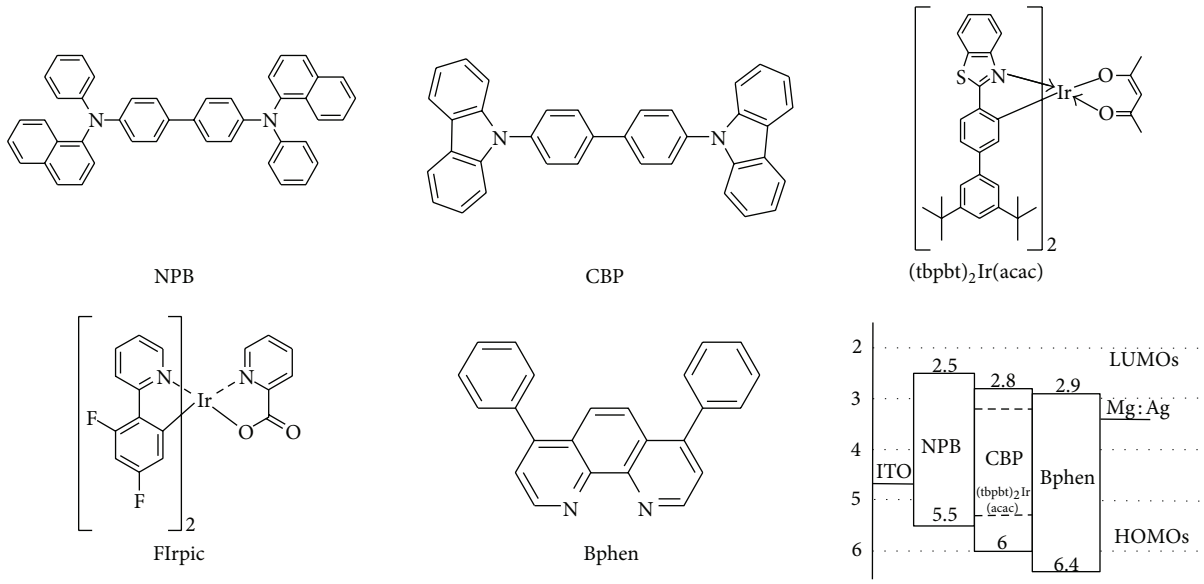

Figure 1: Molecular structures of organic materials and energy level diagram of orange OLEDs in this paper.

However, due to the concentration-sensitive property of most existing phosphorescent dyes, most of existent organic light-emitting devices (OLEDs) only display high performance on the basis of doping system within a narrow doping range from 5 wt% to 10 wt% [8–10]. Therefore, highly efficient concentration-insensitive phosphors, which can hold steady and high efficiency within a relatively wide range of doping ratio, are greatly desired.

Recently, we have reported a novel orange phosphorescent emitter, bis[2-(3′,5′-di-tert-butylbiphenyl-4-yl)benzothiazolato-N,$C^{2'}$]iridium(III) (acetylacetonate) [$(tbpbt)_2Ir(acac)$], which showed a promising quench-resistance property. To further demonstrate its good and stable electroluminescent (EL) performance within a wide doping ratio range, in this study, OLEDs based on $(tbpbt)_2Ir(acac)$ as a light emissive material with different doping concentrations have been fabricated. Moreover, we applied this phosphor as a spectral tailor by fabricating WOLEDs with varied doping ratio, demonstrating that device spectra could be significantly altered without significantly sacrificing device efficiency.

2. Experimental

Prior to the deposition of functional layers, indium tin oxide (ITO) anode substrate with a sheet resistance of 15 Ω/sq was ultrasonically cleaned with detergent, deionized water, acetone, and ethanol, for 15 min at each step. After that, ITO anodes were dried by nitrogen gas flow and subsequently treated with oxygen plasma for 5 min for increasing work function. Organic materials were thermoevaporated with a deposition speed of 0.5 ~ 2 Å/s, at a pressure on the order of magnitude 10^{-4} Pa. After that, metal cathode was fabricated without breaking the vacuum. Film thicknesses and deposition rates were controlled by oscillating quartz thickness monitors. The chemical structures of organic materials and energy level diagram of the OLEDs in this study are shown in Figure 1. It is necessary to explain that the newly synthesized $(tbpbt)_2Ir(acac)$ possesses a quench-resistant property, which permits an optimized doping ratio as high as 20 wt%. The extraordinary property of $(tbpbt)_2Ir(acac)$ along with its chemistry explanations will be reported elsewhere.

Luminance-bias voltage-current density characteristics of devices were measured simultaneously by connecting a spectrometer with a Keithley 4200 semiconductor characterization system. Electroluminescent (EL) spectra and Commission Internationale de l'Eclairage (CIE) (1931) coordinates were tested by an OPT-2000 spectrometer. UV-visible absorption spectra were measured with a Shimadzu UV-1700 spectrophotometer. All the tests were carried out at room temperature in ambient circumstance. The highest occupied molecular orbital (HOMO) and lowest unoccupied molecular orbital (LUMO) energy levels of $(tbpbt)_2Ir(acac)$ were calculated to be −5.29 eV and −3.17 eV, respectively, based on the cyclic voltammetry data and the lowest-energy absorption edge of the UV-vis absorption spectra [11].

3. Results and Discussion

To investigate the concentration-insensitive property of $(tbpbt)_2Ir(acac)$, the first set of devices, that is, ITO/N, N′-diphenyl-1,1′-biphenyl-4,4′-diamine (NPB) (30 nm)/4,4′-N,N′-dicarbazole-biphenyl (CBP) : $(tbpbt)_2Ir(acac)$ (30 nm, *X* wt%)/4,7-diphenyl-1,10-phenanthroline (Bphen) (40 nm)/Mg : Ag, were fabricated, where *X* wt% represented 15 wt% for device A1, 18 wt% for device A2, 20 wt% for device A3, 23 wt% for device A4, and 25 wt% for device A5. Figure 2 depicts the luminance-bias voltage-current density (L-V-J) characteristics of devices A1, A2, A3, A4, and A5. As for the J-V characteristics, it is discernible that the current densities of the devices with higher doping concentration are lower, which

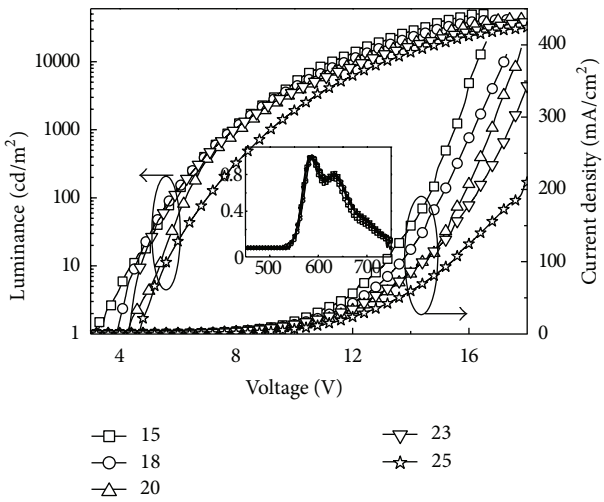

Figure 2: Luminance-bias voltage-current density characteristics of devices A1, A2, A3, A4, and A5. Inset: EL spectra of devices A1-5 at voltage of 8 V. Note that the numbers in the legend represent concentration of $(tbpbt)_2Ir(acac)$ dopant in the devices.

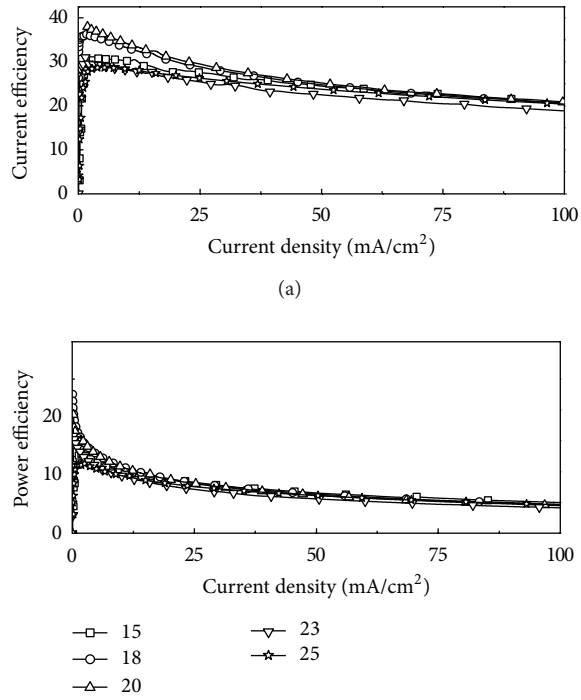

Figure 3: Current efficiency-current density characteristics of devices A1, A2, A3, A4, and A5 (a) and power efficiency-current density characteristics of the devices (b).

should be attributed to the trap effect of $(tbpbt)_2Ir(acac)$ molecule [12, 13]. In addition, the reduction trend of current also indicates that trap effect of the $(tbpbt)_2Ir(acac)$ is greatly dependent on dopant concentration. According to the energy diagram of Figure 1, the HOMO and LUMO offset between $(tbpbt)_2Ir(acac)$ and host CBP is 0.8 eV and 0.5 eV, respectively. As a result, the large energy level offset would trap charge carriers and thus reduce current density. This mechanism will become intensified in device with higher doping ratio due to that more trap sites are provided in these devices. Trap effect of $(tbpbt)_2Ir(acac)$ dopant could be confirmed from the devices maximum luminance and turn-on voltages. It is learned that the maximum luminance of the OLEDs drops with the increase of dopant concentration. A maximum luminance of 50,137 cd/m^2 was realized for device A1 with 15 wt% doping ratio, while gradually decreased with increasing $(tbpbt)_2Ir(acac)$ concentration, corresponding to 41,328 cd/m^2 for device A2, 42,200 cd/m^2 for device A3, 39,947 cd/m^2 for device A4, and 33,532 cd/m^2 for device A5. As for the turn-on voltage, it is exhibited that higher driving voltages are required for devices with higher doping ratio, for example, 3.3 V for device A1, 3.9 V for device A2, 4.4 V for device A3, and 4.4 V for device A4, 4.7 V for device A5. As above discussed, trap effect of Ir-based dopant would be extremely intensified with incremental concentration, which significantly prevents carriers from injecting and transporting in the device to generate current density. Therefore, a higher driving voltage is required in the devices with higher doping ratio to produce equivalent luminance.

The current efficiency-current density characteristics of devices A1, A2, A3, A4, and A5 are depicted in Figure 3(a), and representative data are listed in Table 1. It is depicted that maximum current efficiency of devices with different doping concentration is comparable, that is, 30.8 cd/A for device A1, 36.3 cd/A for device A2, 37.9 cd/A for device A3, 31.0 cd/A for device A4, and 29.3 cd/A for device A5. From Table 1, the largest current efficiency offsets among devices A1, A2, A3, A4, and A5 driven by the same current densities of 10 mA/m^2, 50 mA/m^2, and 100 mA/m^2 are 5.8 cd/A, and 2.3 cd/A, 1.7 cd/A, respectively. If we define efficiency fluctuation rate of varied doped devices driven by a certain current density as

$$\text{Fluctuation Rate } \left(F_{\text{current density}}\right) = \frac{\text{the largest current efficiency offsets}}{\text{largest current efficiency}}, \quad (1)$$

then current efficiency fluctuation rate of devices at 10 mA/m^2, 50 mA/m^2, 100 mA/m^2 is as small as 17.1%, 9.2%, 8.3%, respectively, indicating great concentration-insensitive property of $(tbpbt)_2Ir(acac)$. As has been demonstrated by us, the small efficiency variations with such a wide range of doping concentration could be ascribed to the existence of bulky and twisted di-tert-butylbiphenyl framework, which is beneficial to significantly increase the intermolecular distance and suppress π-π stacking between the phosphorescent iridium complexes [11]. As a result, a promising alleviation of concentration quenching is expected, and a significant concentration-insensitive property is permitted within a wide range of doping concentration from 15 wt% to 25 wt%.

The above experimental results have successfully demonstrated the trap effect and concentration-insensitive

Table 1: Representative data of devices in this study.

Device	V_{on} (V)	L_{max} (max, cd/m^2)	Current efficiency (cd/A)				Power efficiency (lm/W)				Max EQE	CIE[a]
			Max	@ 10 mA/m^2	@ 50 mA/m^2	@ 100 mA/m^2	Max	@ 10 mA/m^2	@ 50 mA/m^2	@ 100 mA/m^2		
A1	3.3	50137	30.8	30.2	24.8	20.5	13.1	10.2	6.5	5.1	14.9	(0.58, 0.43) (8 V)
A2	3.9	41328	36.3	33.1	24.8	20.6	22.5	10.8	6.5	4.8	17.5	(0.57, 0.43) (8 V)
A3	4.4	42200	37.9	34.0	24.9	20.4	20.8	10.9	6.2	4.5	18.2	(0.57, 0.43) (8 V)
A4	4.4	39947	31.0	28.2	22.6	18.9	17.3	9.4	5.6	4.1	15.1	(0.57, 0.43) (8 V)
A5	4.7	33532	29.3	28.4	23.7	20.2	11.4	9.4	6.1	4.6	14.0	(0.58, 0.42) (8 V)
B1	3.1	36172	29.8	23.7	18.4	15.0	23.8	11.9	6.7	4.8	15.2	(0.30, 0.35) (8 V)
B2	3.1	35505	31.6	27.0	20.3	15.9	27.3	12.3	6.9	4.9	17.1	(0.32, 0.36) (8 V)
B3	3.1	33856	38.8	32.0	22.9	17.4	30.0	13.9	7.3	4.9	18.1	(0.33, 0.37) (4 V) (0.33, 0.37) (6 V) (0.33, 0.36) (8 V) (0.33, 0.36) (10 V) (0.33, 0.36) (12 V) (0.32, 0.36) (14 V)
B4	3.2	23518	40.7	30.8	20.0	15.3	32.2	12.7	6.3	4.3	19.0	(0.43, 0.39) (8 V)
B5	3.6	21099	37.3	31.2	20.3	15.1	23.1	12.7	6.3	4.2	18.1	(0.45, 0.41) (8 V)

V_{on}: turn-on voltage, L_{max}: maximum luminance, EQE: external quantum efficiency, CIE: Commission Internationale de l'Eclairage coordinates.
[a]Data in parentheses are the corresponding driven voltages.

property of $(tbpbt)_2Ir(acac)$ with a wide range of doping ratio. Meanwhile, the EL spectra of the devices imply that $(tbpbt)_2Ir(acac)$ might be a suitable orange phosphor to fabricate orange-plus-blue WOLEDs. To further explore its potential application in tailoring device EL spectrum and efficiency, another set of devices, WOLEDs combining $(tbpbt)_2Ir(acac)$ orange layer with a bis(4,6-(difluorophenyl)pyridinato-N,$C^{2'}$)picolinate iridium(III) (FIrpic) doped sky-blue layer, have been fabricated. The device structure is ITO/NPB (30 nm)/CBP : FIrpic (20 nm, 8 wt%)/CBP : $(tbpbt)_2Ir(acac)$ (10 nm, X wt%)/Bphen (40 nm)/Mg : Ag, where X wt% represents 15 wt% for device B1, 18 wt% for device B2, 20 wt% for device B3, 23 wt% for device B4, and 25 wt% for device B5. The concentration of FIrpic was optimized according to our previous work [8–10]. Figure 4 shows the luminance-bias voltage-current density characteristics of devices B1, B2, B3, B4, and B5. Compared with EL behaviors of the monochrome devices, similar trend was obtained by WOLEDs, once again confirming our inference about the trap effect and concentration-insensitive property of $(tbpbt)_2Ir(acac)$ phosphor. As for the J-V characteristics of devices with varied doping concentration, the current densities are observed to reduce with the incremental dopant concentration, revealing the trap effect of $(tbpbt)_2Ir(acac)$ in our devices. From the L-V characteristics, it is shown that the maximum luminance of the OLEDs drops with the increased dopant concentration. A maximum luminance of 36,172 cd/m^2 was realized for device B1 with 15 wt% doping ratio, while gradually decreased with increasing the doping ratio, corresponding to 35,505 cd/m^2 for device B2, 33,856 cd/m^2 for device B3, 23,518 cd/m^2 for device B4, and to 21,099 cd/m^2 for device B5. As for the turn-on voltage, it is learned that devices with lower doping ratio exhibit the smaller bias, that is, 3.1 V for device B1, 3.1 V for device B2, 3.1 V for device B3, 3.2 V for device B4, and 3.6 V for device B5.

Figure 5 depicts the EL spectra of devices B1, B2, B3, B4, and B5. Two emission peaks could be located at ~470 nm (along with a shoulder at ~490 nm) and ~580 nm (along with a shoulder at ~630 nm), originating from the emission of FIrpic-doped layer and $(tbpbt)_2Ir(acac)$-doped layer, respectively. With relatively lower doping ratio, devices B1 and B2 exhibit a blue-dominant emission, indicating that most electrons could travel through orange emitting layer (EML) and ultimately recombine with holes in FIrpic layer. With the increased doping ratio, blue emission is gradually suppressed, implying that trap effect of the $(tbpbt)_2Ir(acac)$ phosphor could hinder electrons from injecting into FIrpic-doped layer. Two reasons should be related to the dominant emission of orange EML in devices with high $(tbpbt)_2Ir(acac)$ doping ratio. (1) As discussed above, higher doping ratio would greatly intensify trap effect of the dopant; consequently, more excitons would be generated and utilized in orange EML. (2) higher doping ratio would provide more emitters in devices, which could also facilitate exciton utilization and light emission in orange EML. CIE coordinates of the devices shift from (0.30, 0.35) for device B1 to (0.45 0.41) for device B5 (detailed data are shown in Table 1). Balanced white emission is achieved in device B3 with 20 wt% $(tbpbt)_2Ir(acac)$ doping ratio. Thereby, the spectra of device B3 at different driving voltages are shown in inset of Figure 5. It is exhibited that the EL spectra display negligible dependence on the bias voltage. Meanwhile, with the increase of the bias, the CIE coordinates of the white emission slightly vary from (0.33, 0.37) at 4 V

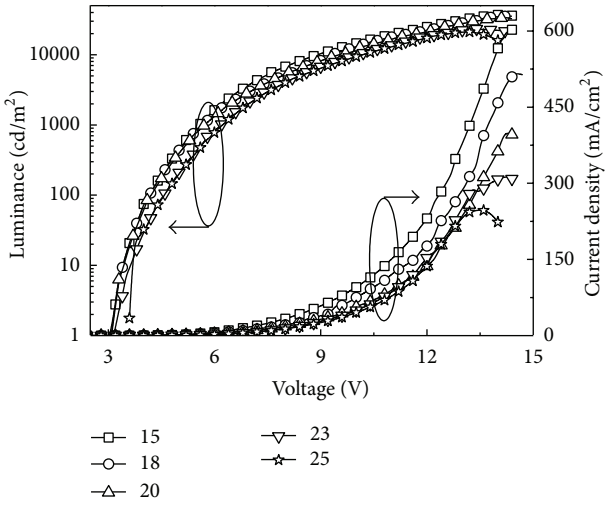

Figure 4: Luminance-bias voltage-current density characteristics of devices B1, B2, B3, B4, and B5.

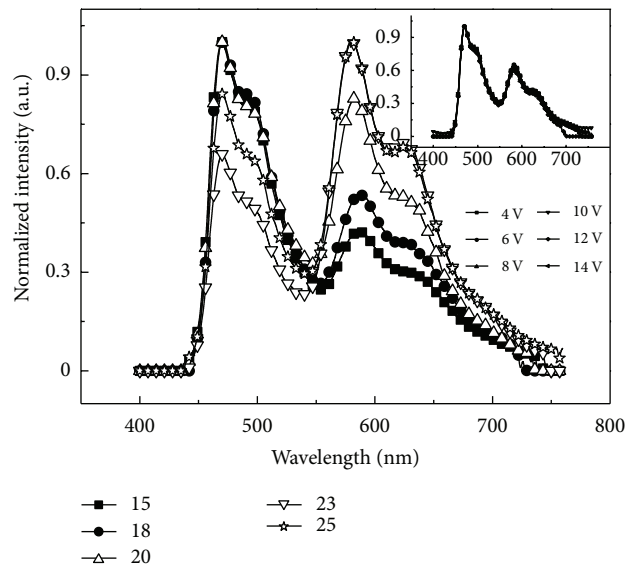

Figure 5: EL spectra of devices B1, B2, B3, B4, and B5 at bias voltage of 8 V. Inset: EL spectra of device B3 driven by different bias voltages.

to (0.32, 0.36) at 14 V, which are very close to the ideal CIE coordinates for pure white light.

The current efficiency-current density characteristics of devices B1, B2, B3, B4, and B5 are depicted in Figure 6(a), and representative data are listed in Table 1. Owing to the concentration-insensitive characteristics of $(tbpbt)_2Ir(acac)$, current efficiency and power efficiency of varied doping WOLEDs are comparable at the same current densities. Current efficiency fluctuation rates of devices at 10 mA/m^2, 50 mA/m^2, and 100 mA/m^2 are 25.9%, 19.6%, and 13.8%, respectively. Among these devices, device B3 with doping concentration of 20 wt% shows the maximum peak luminance efficiency, power efficiency, and EQE of 38.8 cd/A, 30.0 lm/W, and 18.1%, respectively. The performance of our

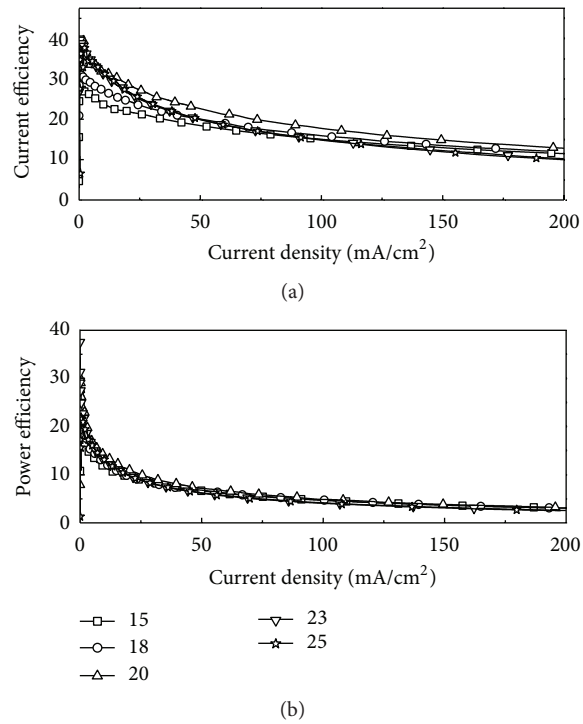

Figure 6: Current efficiency-current density characteristics of devices B1, B2, B3, B4, and B5 (a) and power efficiency-current density characteristics of the devices (b).

present WOLEDs is comparable or even better than that of many lightly doped devices, and the comparable efficiency behaviors of WOLEDs reveal a promising application of the concentration-insensitive phosphor. So far, although technique of altering doping ratio has been widely accepted to adjust device spectra, the optimization of device parameters is tedious and time-consuming because doping ratio variations could also induce device efficiency alteration. Our work should be very meaningful due to that the optimization process can be greatly simplified due to concentration-insensitive property of $(tbpbt)_2Ir(acac)$.

4. Conclusion

In conclusion, by employing a novel iridium complexes material of $(tbpbt)_2Ir(acac)$ as the emitter, highly efficient phosphorescent OLEDs with orange color emission were obtained with a wide range of doping concentration, suggesting that $(tbpbt)_2Ir(acac)$ could serve as the promising concentration-insensitive orange phosphor. Meanwhile, the unique characteristic was applied to fabricate white OLEDs with a wide doping ratio range, demonstrating that $(tbpbt)_2Ir(acac)$ could effectively tailor spectral color without obviously sacrificing device efficiency.

Acknowledgments

This work was supported by the National Science Foundation of China (NSFC) (Grant nos. 61177032 and 61006036), the

Foundation for Innovative Research Groups of the NSFC (Grant no. 61021061), the Fundamental Research Funds for the Central Universities (Grant nos. ZYGX2010Z004), SRF for ROCS, SEM (Grant no. GGRYJJ08-05), Doctoral Fund of Ministry of Education of China (Grant no. 20090185110020).

References

[1] S. Reineke, F. Lindner, G. Schwartz et al., "White organic light-emitting diodes with fluorescent tube efficiency," *Nature*, vol. 459, no. 7244, pp. 234–238, 2009.

[2] J. Kido, M. Kimura, and K. Nagai, "Multilayer white light-emitting organic electroluminescent device," *Science*, vol. 267, no. 5202, pp. 1332–1334, 1995.

[3] Q. Wang, J. Ding, M. Dongge et al., "Harvesting excitons via two parallel channels for efficient white organic LEDs with nearly 100% internal quantum efficiency: fabrication and emission-mechanism analysis," *Advanced Functional Materials*, vol. 19, no. 1, pp. 84–95, 2009.

[4] G. Zhang, H. H. Chou, X. Jiang, P. Sun, and C. H. Cheng, "Highly efficient white organic light-emitting diodes based on broad excimer emission of iridium complex," *Organic Electronics*, vol. 11, no. 7, pp. 1165–1171, 2010.

[5] G. Xie, Z. Zhang, Q. Xue et al., "Tailoring the efficiencies and spectra of white organic light-emitting diodes with the interlayers," *Journal of Physical Chemistry C*, vol. 115, no. 1, pp. 264–269, 2011.

[6] S. M. Chen, G. P. Tan, W. Y. Wong, and H. S. Kwok, "White organic light-emitting diodes with evenly separated red, green, and blue colors for efficiency/color-rendition trade-off optimization," *Advanced Functional Materials*, vol. 21, no. 19, pp. 3785–3793, 2011.

[7] T. Inden, T. Hishida, M. Takahashi, M. Ohsumi, and N. Ohtani, "White organic light-emitting diodes using two phosphorescence materials in a starburst hole-transporting layer," *International Journal of Photoenergy*, vol. 2012, Article ID 703496, 7 pages, 2012.

[8] J. S. Yu, X. Lei, R. Jiang, and J. Zhao, "Influence of interlayer on the performance of phosphorescent white organic light-emitting devices," *Displays*, vol. 33, no. 3, pp. 142–145, 2012.

[9] H. Sasabe, J. I. Takamatsu, T. Motoyama et al., "High-efficiency blue and white organic light-emitting devices incorporating a blue iridium carbene complex," *Advanced Materials*, vol. 22, no. 44, pp. 5003–5007, 2010.

[10] F. F. Yu, H. L. Fan, H. F. Huang et al., "Blue fluorescence from the ligand and yellow phosphorescence from the iridium complex: high-efficiency wet-processed white organic light-emitting device," *Inorganica Chimica Acta*, vol. 390, no. 15, pp. 119–122, 2012.

[11] M. Li, H. Zeng, Y. Meng et al., "Fine tuning of emission color of iridium(iii) complexes from yellow to red via substituent effect on 2-phenylbenzothiazole ligands: synthesis, photophysical, electrochemical and DFT study," *Dalton Transactions*, vol. 40, no. 27, pp. 7153–7164, 2011.

[12] B. D. Chin, M. C. Suh, M. H. Kim, S. T. Lee, H. D. Kim, and H. K. Chung, "Carrier trapping and efficient recombination of electrophosphorescent device with stepwise doping profile," *Applied Physics Letters*, vol. 86, no. 13, Article ID 133505, pp. 1–3, 2005.

[13] S. O. Jeon, S. E. Jang, H. S. Son, and J. Y. Lee, "External quantum efficiency above 20% in deep blue phosphorescent organic light-emitting diodes," *Advanced Materials*, vol. 23, no. 12, pp. 1436–1441, 2011.